Artigo

INVESTIGATING THE SPONTANEOUS FORMATION OF SDS MICELLE IN AQUEOUS SOLUTION USING A COARSE-GRAINED FORCE FIELD

José Maria Pires*
Departamento de Física, Universidade Federal do Espírito Santo, Av. Fernando Ferrari, 514, Campus de Goiabeiras, 29075-910 Vitória – ES, Brasil
André F. de Moura e Luiz C. G. Freitas
Departamento de Química, Universidade Federal de São Carlos, Rod. Washington Luiz, km 235, 13565-905 São Carlos – SP, Brasil

A 1μs Molecular Dynamic simulation was performed with a realistic model system of Sodium Dodecyl Sulfate (SDS) micelles in aqueous solution, comprising of 360 DS⁻, 360 Na⁺ and 90000 water particles. After 300 ns three different micellar shapes and sizes 41, 68 and 95 monomers, were observed. The process led to stabilization in the total number of SDS clusters and an increase in the micellar radius to 2.23 nm, in agreement with experimental results. An important conclusion, is be aware that simulations employed in one aggregate, should be considered as a constraint. Size and shape distribution must be analyzed.

Keywords: SDS; MDS; Coarse-Grained.

INTRODUCTION

Is well known that surfactants in water can self assemble readily to form a large variety of aggregates, including micelles. In the last two decades, Molecular Dynamic (MD) simulations have become a preferential tool in the investigation of micellar systems.[1-16] MD simulations can provide insight into structural and dynamical features of assembled molecules but the inherent complexity of the systems and an accurate description of structural and dynamic features require elaborate modeling and adequate system size. Otherwise, the long relaxation times involved in self-assembling impose some limitations on the detailed study of aggregation processes using this methodology.[1]

The traditional approach is use the atomistic all atoms (AA) model to represent explicitly the system, however, because of their computational cost, the amount of water and surfactants molecules tends to be reduced. To overcome these difficulties many coarse-grained models have been proposed.[17-20] Among the propositions the MARTINI Corse-Grained Force Field allows computer simulations to be run on length and time scales that are 2-6 orders of magnitude larger compared to atomistic simulations.[21-24] Besides the proposition of coarse-grained models, hybrid methodologies have been proposed to study large micellar systems.[25-27] More recently, implicit solvent model using dissipative particle dynamics (DPD) and Monte Carlo (MC),[28,29] have been carried out. We chose the MARTINI CG model, because of the simplicity of it. Only a small number of coarse grained atom types are defined, which interact using a few discrete levels of interaction. Despite the computational speed and the simplistic nature of the model, it proves to be both versatile in its applications and accurate in its predictions.

In the present work a 1μs MD trajectory of the Sodium Dodecyl Sulfate (SDS) in water was obtained using the MARTINI force field. This trajectory was long enough to observe the self- assembling of monomers, and therefore, it is possible to compare the sizes, geometries and number of these micellar aggregations with experimental data and other works of molecular dynamic simulations. Although, the SDS micelle has been extensively studied,[26,27,30-37] to the best of

our knowledge this is the first time that a microsecond trajectory has been calculated, allowing the spontaneous SDS micellization to be observed. Therefore, as will be discussed, the trajectory obtained shown details of the micellar formation not revealed by experimental data, once the measured results are an average over all aggregates.

EXPERIMENTAL

The standard MARTINI force field version 2.0 parameters have already been used to study vesicle fusion,[21] DPC micelle (54 monomers), DPPC bilayer (1600 monomers)[22] and DPPC/Cholesterol system.[23] In the present study, each dodecyl sulfate was represented by one hydrophilic head group, type Qa, with a charge of -1 and 96 amu and three hydrophobic particles (C1, C2 and C3), each one representing four CH2 / CH3 units with 56 amu. Sodium ions were represented by a CG particle of the type Qd, with a charge of +1, which is equivalent to a hydrated sodium ion. Four real waters molecules were represented by one CG water, type P4.

Our model system consisted of 360 anionic species and 360 Na⁺ counter ions surrounded by 90000 water particles. The experimental SDS CMC is 8 mM[33] and the present concentration is 55 mM, high enough to ensure the self assembling. To obtain the initial system configuration the dodecyl sulfate, Na⁺ and water particles were placed at random into a cubic box with the edge size of 25.0 nm. Repulsive contacts were avoided using a 0.47 nm cutoff.

Simulations were carried out in the NpT ensemble using the GROMACS 3.3.3 package.[38,39] The weak coupling scheme of Berendsen[40] was used for the temperature (300 K, τ_T = 0.1 ps) and isotropic pressure (1 bar, τ_p = 0.2 ps), 3.0 x 10⁵ bar⁻¹ of compressibility), coupling each component to a separate heat bath. Lennard-Jones and Coulomb interactions were cut off at 1.2 nm, with a shift function applied to the Lennard-Jones at 0.9 nm and a dielectric constant equal to 15. The smooth particle-mesh Ewald method was used to evaluate long-range electrostatic interactions.[41] The trajectory was integrated up to 1μs in the constant NpT ensemble, using a time step of 40 fs. The neighbor list was updated every tenth step and the configuration of the system was saved every 100ps. The calculation was performed on a dedicated Dual Quad Xeon E5410/2.33 GHz running the Arch Linux 2009 operational system.

*e-mail: piresufes@yahoo.com.br

RESULTS AND DISCUSSION

At the beginning of the simulation small aggregates started to be formed and the system relaxation occurred within 250 ns approximately. See Figure 1S, supplementary material. Aggregates with 40 monomers could be observed between 70 ns and 98 ns, increasing to a ca. 70 after this time. This persists till simulation time of 225 ns. These formation and breaking of SDS micelles can be followed by visual inspection of Figure 1.
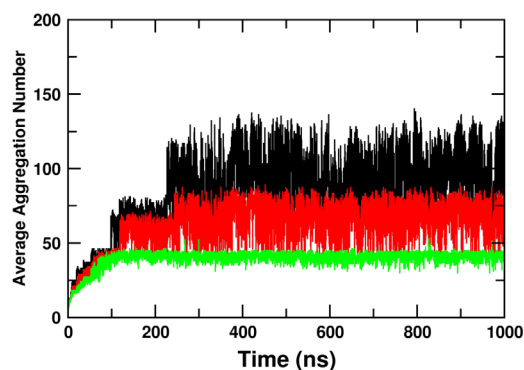

Figure 1. Aggregation number of the micellar aggregates. Showing the largest aggregates

After t=225 ns a new jump occurs in the micelle formation and N goes to 110. One can observe that after initial relaxation, the number of aggregates remained most of the time around 6. During the last 600 ns of the simulation we could compute three major groups of aggregates with different sizes $< N > = 41 \pm 3$, 68 ± 10 and 95 ± 17 (Figure 1). These information can not be obtained from the experimental data as the measured results are an average over all aggregates. Furthermore, it is worth pointing out the dynamic nature of this process as micelles are being created.

Figure 2S, supplementary material, describes the aggregates sizes distribution with characteristic peaks of monomers formation at N = 39, 76 and 108. The average micellar size may be computed from the simulation, taking into account the aggregation number and the radius of gyration of the SDS clusters at each step. Considering aggregates larger than N=5 at each moment of the trajectory, a clear indication that a large structural rearrangement occurred in the first 250 ns of the simulation, characterized by an increase in the values of the aggregation number (Figure 1), the average cluster size (Figure 3S, supplementary material) and the average radius of gyration (R_G) (Figure 4S, supplementary material), was observed. The behavior of the average number of aggregation, $< N >$, as the simulation proceeds, was obtained taking the last 600 ns of the simulation.

Figure 2 shows a series of snapshots illustrating a fusion and a quasi-fusion process. Water particles are not shown for clarity. Starting from a random distribution at 0 ns, the approximation of two micelles with N = 46 and N = 26 occurred at 189.8 ns. At 192.0 ns, these two micelles formed a large micelle with N = 72. At 257.6 ns a micelle with 45 monomers approximated of the previous one (N = 72), to aggregate at 260.0 ns, forming an even larger micelle with N = 117 monomers. At t=399.6 ns, a quasi-fusion, was observed when a micelle with N = 63 spent 0.2 ns near the N = 117 micelle. The next snapshots show the structure at 500 ns and the end of the simulation at 1μs. These aggregates did not change considerably in the last 500 ns of the simulation. By visual inspection of the trajectory animation, it is clear that small micelles (N < 70) are spherical, medium size ones (N >100 N > 70) have a prolate ellipsoidal shape and the large ones (N > 100) may be viewed as worm-like.
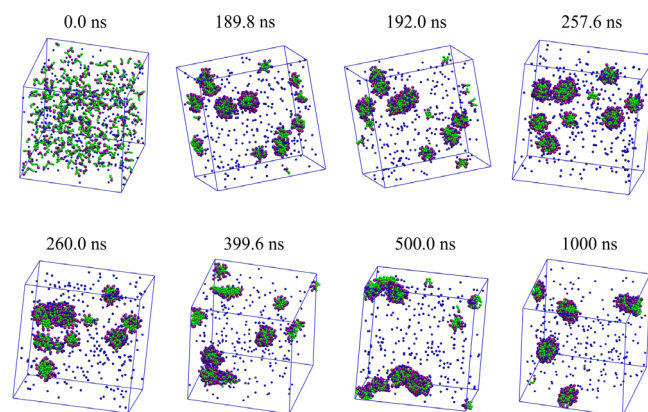

Figure 2. Spontaneous aggregation of SDS surfactants into micelles at 55 mM concentration. Head groups are drawn in purple, tails in green, counterions in blue. Water is omitted for clarity

The radial distribution of the sodium ion around the sulfates head groups can be observed in Figure 3, presenting a peak at r = (0.50 ± 0.03) nm.
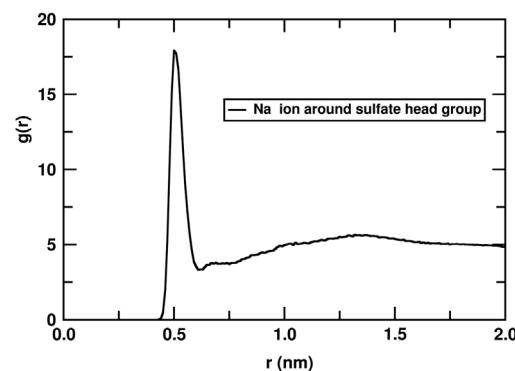

Figure 3. Radial distribution function of Na ion around sulfate ion

By evaluating the number of sodium ions around the polar sulfates at the correlation peak, a density value of 0.98 mol/L of Na^+ was obtained. It is important to remind that the average concentration of Na^+ is 0.055 mol/L. After the first coordination shell of the sodium ions around the SO_4^- groups, begin a region formed by water and Na^+ ion, called diffuse region. At the diffuse region the density of sodium ions around the polar sulfates values drops to 0.30 mol/L. having a peak at 1.33 nm and extending until 7.0 nm (not shown in the graphic). The peak and extension of the diffuse region values computed by us are in good agreement with the experimental data reported by Joshi *et al.*[42] as well as with the theoretical result by Bruce *et al.*.[34] The coordination number of Na^+ ion around the sulfate head group was equal 0.76 and the residence time was equal to 135 ps.

The same analysis was done for water around sodium ion and sulfate head groups (Figure 4). By observing the distribution of water around the Na^+ ion, it is possible to identify three coordination shells: a very well structured at r = (0.52 ± 0.04) nm a second at r = 0.98 nm and third at r = 1.38 nm. The water distribution in these shells is: 0.73, 0.26 and 0.24 mol/L, respectively.

The coordination number of water around Na^+ was equal to 12 in the first coordination shell and the water residence time is equal to 58 ps. The water distribution around the sulfates head groups follows the same pattern, but lower densities were obtained: 0.52, 0.20 and 0.16 mol/L, respectively. The coordination number of water around the SO_4^- groups is equal to 9 and the residence time was 57 ps.
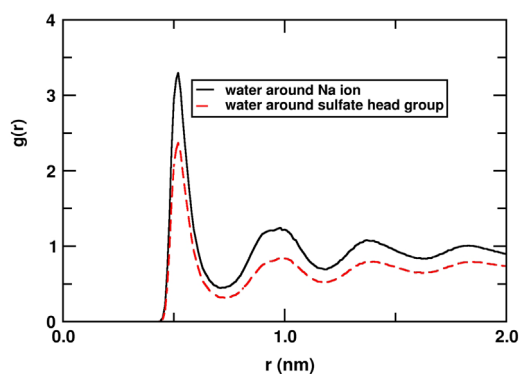
Figure 4. Radial distribution function of water molecules around the Na ion (black line) and sulfate ion (red line)

Figure 5 shows the radial distribution of water around C1, C2 and C3 coarse-grained sites. All values lie below unity, indicating the low probability of finding water particles near hydrophobic sites. The low densities of water close to these groups, agrees with the information[34-37] that there is no hydration inside the SDS micelles.
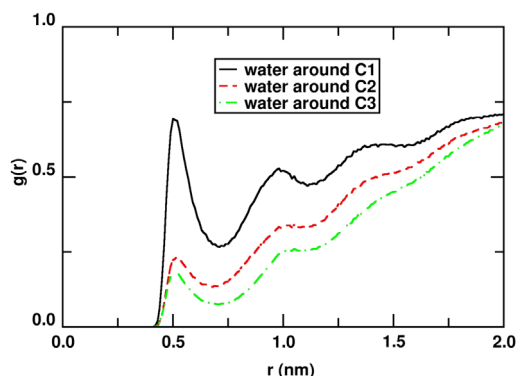

Figure 5. Radial distribution function of water molecules around the C1, C2 and C3 groups. Black, red and green lines, respectively

The behavior of the Lennard–Jones and Coulomb energies between the Dodecyl Sulfates (DS^- - DS^-) are shown in Figure 6 and Figure 5S, supplementary material. The average value of the Lennard-Jones energy between 500.0 and 1000 ns was (-15200 ± 300) kJ/mol, while the Coulomb energy was (+772 ± 36) kJ/mol. The steps observed in the Lennard-Jones energy may be ascribed to fusion and quasi-fusion processes.
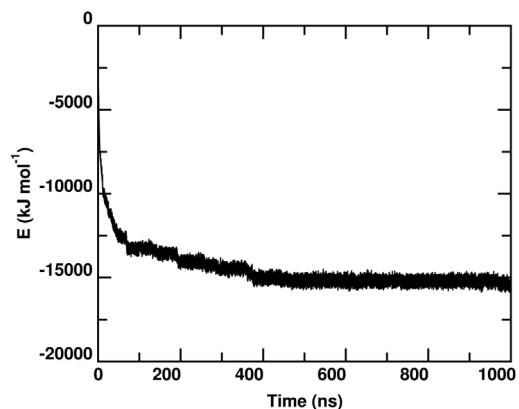

Figure 6. Lennard-Jones energy between DS^- anion from 0.0 up to 1000 ns simulation

Figure 7 shows the Coulomb energy between Dodecyl sulfate and sodium around 399.6 ns. The average Coulomb energy between 360.0 and 440.0 ns was -1400 kJ/mol, whereas at t = 399.6 ns it was -1690 kJ/mol, showing the importance of salt bridges during the fusion process to form new micelles.
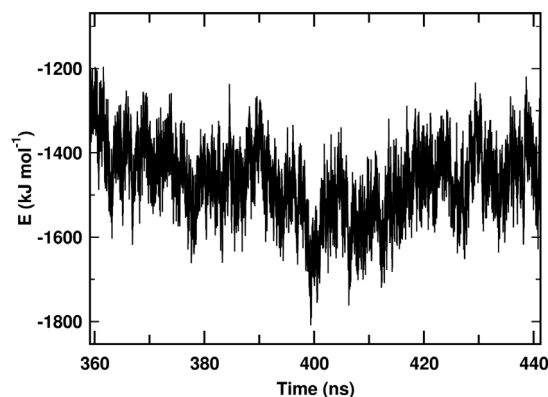

Figure 7. Detail of the DS^- anion and Na^+ cation Coulomb energy at t = 399.6 ns during a quasi-fusion process

In Table 1S, supplementary material, we present the experimental and theoretical data about SDS micelle and compare with our CG calculation. The measurements were performed in aqueous solution with small angle neutron scattering (SANS) experiments[42-47] and small angle X-ray scattering (SAXS).[42,47,48] As have been discussed, better experimental characterizations are obtained using both techniques.[42-47] The SANS is used to study the hydrophobic region and the SAXS to analyze the head group thickness and the counter ion condensation region. This procedure gives much more reliable information about the micellar structure. The experimental data selected by us have SDS concentration close to 55 mM, except the one from ref. 50 measured at 300 mM. We also reported the average aggregation number < N > and the average micellar radius < R >. It is important to remind that frequently, more than one theoretical model can be used to analyze a given data set. Therefore, in Table 1S are shown results obtained using different models. Molecular Dynamics results for the SDS obtained using all atoms force field, coarse-grain and hybrid models are also compared with the present CG results.

In spite of our simulation has considered all possible aggregates and shapes, the average micellar radius calculated in the trajectory interval between 600 and 1000 ns was (2.23 ± 0.08) nm, in agreement particularly with those derived from polydisperse spheres.[43,45,46]

In the SDS simulations reported by Bruce *et al.*[34] and Jalili *et al.*[37] only one aggregate could be formed and therefore the micellar size was constrained by the simulation conditions. In these studies, estimations of micellar size were based on the average position of the head group atoms or on the radius of gyration and the results obtained are also in agreement with experimental data (Table 1S, supplementary material).

The fact that the larger model system employed here yielded an average micelle size comparable to the ones reported in those previous studies, shows that great care must be taken in interpreting the simulation results. As have been discussed before different micellar sizes were reported by averaging aggregates with different number of monomers.[42-48] Therefore, regarding the micellar radius, sound conclusions can be obtained if the size distribution is taken into account. The histogram of the number of aggregates in Figure 1S, supplementary material, shows a polydisperse system with various overlap populations, it is not correct to speak of an average when there are several distinct populations to be evaluated.

CONCLUSIONS

Results, from a large-scale MARTINI Coarse-Grained Force Field Molecular Dynamics simulation of SDS micellar system have been presented. The simulation run (1 μs) was long enough to promote the self-assembling of the monomers showing the prevalence of three different sizes $< N > = 41 \pm 3$, $< N > = 68 \pm 10$, and $< N > = 95 \pm 17$. In this way, micelle-micelle and micelle-monomer interactions were taken explicitly into account. The micelle size distribution changed over the course of the simulation due to the exchange and fusion of monomers, which led to the presence of small, large and very large aggregates, with a large variety of shapes too. It was possible discover that these aggregates are hidden in the experimental data, once the experiments shows only the average aggregates sizes. In spite of this, the average micellar sizes obtained are in agreement with experimental results. Evaluating the Coulomb energy between Dodecyl Sulfate anion and Sodium cation, show the importance of salt bridges between aggregates during the fusion process to form new micelles.

The present results indicate that these clusters are stable in the 1 μs scale. These finds reinforce once more the necessity of micellar molecular dynamic simulations goes to the μs scale of time. Nowadays this is a reachable objective, using coarse-grained models for simulations.

Another important conclusion, is be aware that simulations employed in one aggregate, should be considered as a constraint. They must be handled with care, taking into account the size and shape distribution.

SUPPLEMENTARY MATERIAL

The supplementary material is available in http://quimicanova. sbq.org.br, with free access at pdf file.

ACKNOWLEDGMENT

REFERENCES

1. Shelley, J. C.; Shelley, M. Y.; *Curr. Opin. Colloid Interface Sci.* **2000**, *5*, 101.
2. Jönsson, B.; Edholm, O.; Teteman, O.; *J. Chem. Phys.* **1986**, *85*, 2259.
3. Watanabe, K.; Ferrario, M.; Klein, M. L.; *Phys. Chem.* **1988**, *92*, 819.
4. Watanabe, K.; Klein, M. L.; *J. Phys. Chem.* **1989**, *93*, 6897.
5. Shelley, J.; Sprik, M.; Klein, M. L.; *Langmuir* **1993**, *9*, 916.
6. Kuhn, H.; Rehage, H.; Bunsen, B.; *Phys. Chem.* **1997**, *101*, 1485.
7. Laaksonen, L.; Rosenholm, J. B.; *Chem. Phys. Lett.* **1993**, *216*, 429.
8. de Moura, A. F.; Freitas, L. C. G.; *Braz. J. Phys.* **2004**, *34*, 64.
9. Bast, T.; Hentschke, R.; *J. Phys. Chem.* **1996**, *100*, 12162.
10. Wymore, T.; Gao, X. F.; Wong, T. C.; *J. Mol. Struct.* **1999**, *485-486*, 195.
11. Bogusz, S.; Venable, R. M.; Pastor, R. W.; *J. Phys. Chem. B* **2000**, *104*, 5462.
12. Tieleman, D. P.; van der Spoel, D.; Berendsen, H. J. C.; *J. Phys. Chem. B* **2000**, *104*, 6380.
13. Balasubramanian, S.; Bagchi, B.; *J. Phys. Chem. B* **2000**, *106*, 3668.
14. Mailet, J. B.; Lachet, V.; Coveney, P. V.; *Phys. Chem. Phys.* **1999**, *1*, 5277.
15. de Moura, A. F.; Freitas, L. C. G.; *Chem. Phys. Lett.* **2005**, *411*, 474.
16. Marrink, S. J.; Tieleman, D. P.; Mark, A. E.; *J. Phys. Chem. B* **2000**, *104*, 12165.
17. Baschnagel. J.; Binder, K.; Paul, W.; Laso, M.; Suter, U. W.; Batoulis, I.; Jilge, W.; *Phys. Chem.* **1991**, *95*, 6014.
18. Schweizer, K. S.; David, E. F.; Singh, C.; Curro, J. G.; Rajasekaran, J. J.; *Macromolecules* **1995**, *28*, 1528.
19. Samanta, S. K.; Bhattacharya, S.; Maiti, P. K.; *J. Phys. Chem. B* **2009**, *113*, 13545.
20. DeMille, R. C.; Molinero, V.; *J. Chem. Phys.* **2009**, *131*, 34107.
21. Marrink, S. J.; Mark, A. E.; *J. Am. Chem. Soc.* **2003**, *125*, 11144.
22. Marrink, S. J.; Mark, A. E.; *J. Phys. Chem. B* **2004**, *108*, 750.
23. Marrink, S. J.; Risselada, H. J.; Yefimov, S.; Tieleman, D. P.; de Vries, A. H.; *J. Phys. Chem. B* **2007**, *111*, 7812.
24. Monticelli, L.; Kandasamy, S. K.; Periole, X.; Larson, R. G.; Tieleman, D. P.; Marrink, S. J.; *J. Chem. Theory Comput.* **2008**, *4*, 819.
25. Lazaridis, T.; Mallik, B.; Chen, Y.; *J. Phys. Chem. B* **2005**, *109*, 15098.
26. Gao, J.; Ge, W.; Hu, G.; Li, J.; *Langmuir* **2005**, *21*, 5223.
27. Gao, J.; Ren, Y.; Ge, W.; *Chin. J. Chem. Eng.* **2009**, *17*, 654.
28. Yamamoto, S.; Maruyama, Y.; Hyodo, S.; *J. Chem. Phys.* **2002**, *116*, 5842.
29. Jusufi, A.; Hynninen, A. P.; Panagiotopoulos, A. Z.; *J. Phys. Chem. B* **2008**, *112*, 13783.
30. Rakitin, A. R.; Pack, G. R.; *J. Phys. Chem. B* **2004**, *108*, 2712.
31. Quina, F. H.; Nassar, P. M.; Bonilha, J. B. S.; Bales, B. L.; *J. Phys. Chem.* **1995**, *99*, 17028.
32. Ikeda, S.; Hayashi, S.; Imae, T.; *J. Phys. Chem.* **1981**, *85*, 106.
33. Croonen, Y.; Geladé, E.; van der Ziegel, M.; van der Auweraer, M.; Vandendriessche, H.; De Schryver, F. C.; Almgren, M.; *J. Phys. Chem.* **1983**, *87*, 1426.
34. Bruce, C. D.; Bekowitz, M. L.; Perera, L.; Forbes, M. D. E.; *J. Phys. Chem. B* **2002**, *106*, 3788.
35. Shelley, J.; Watanabe, K.; Klein, M. L.; *Int. J. Quantum Chem.* (**1990**), DOI: 10.1002/qua.560381713, colocar citação complete após o doi.
36. MacKerell, A.; *J. Phys. Chem.* **1995**, *99*, 1846.
37. Jalili, S.; Akhavan, M.; *Colloids Surf., A* **2009**, *352*, 99.
38. Lindahl, E.; Hess, B.; van der Spoel, D.; *J. Mol. Model.* **2001**, *7*, 306.
39. Berendsen, H. J. C.; van der Spoel, D.; van Drunen, R.; *Comput. Phys. Commun.* **1995**, *91*, 43.
40. van der Spoel, D.; Lindahl, E.; Hess, B.; Groenhof, G.; Mark, A. E.; Berendsen, H. J. C.; *J. Comput. Chem.* **2005**, *26*, 1701.
41. Essman, U.; Perela, L.; Berkowitz, M. L.; Darden, ??; *J. Phys. Chem. B* **2005**, *109*, 15098; Lee, H.; Pedersen, L. G.; *J. Chem. Phys.* **1995**, 103, 8577.
42. Joshi, J. V.; Aswal, V. K.; Goyal, P. S.; *J. Phys.: Condens. Matter* **2007**, *19*, 196219.
43. Hayter, H. J. B.; Penfold, J.; *J. Chem. Soc. Faraday Trans.* **1981**, *77*, 1851.
44. Garg, G.; Hassan, P. A.; Aswal, V. K.; Kulshreshtha, S. K.; *J. Phys. Chem. B* **2005**, *109*, 1340.
45. Chen, S. H.; *Ann. Rev. Phys. Chem.* **1986**, *37*, 351.
46. Bergstrom, M.; Pedersen, J. S.; *Phys. Chem. Chem. Phys.* **1999**, *1*, 4437.
47. Prévost, S.; Gradzielski, M.; *J. Colloid Interface Sci.* **2009**, *337*, 472.
48. Caetano, W.; Gelamo, E. L.; Tabak, M.; Itri, R.; *J. Colloid Interface Sci.* **2002**, *248*, 149.